SIMULATION OF SEMICONDUCTOR DEVICES AND PROCESSES Vol. 3
Edited by G. Baccarani, M. Rudan - Bologna (Italy) September 26-28, 1988 - Tecnoprint

ASWR - Method for the Simulation of Dopant Redistribution in Silicon

J.Lorenz, M.Svoboda

Fraunhofer - Arbeitsgruppe für Integrierte Schaltungen,
Artilleriestraße 12, 8520 Erlangen, Germany

SUMMARY

An Asymmetric Weighted Residual (ASWR) method has been developed for the application in the universal two-dimensional process simulation program COMPOSITE (Lorenz 1985). This approach which is quite similar to Finite Elements includes an adaptive mesh and allows the numerical solution of the system of coupled stiff partial differential equations necessary to describe dopant diffusion in silicon with high accuracy and a small number of meshpoints. In this paper, an outline of the method is given and the implementation in COMPOSITE is described.

INTRODUCTION

For the simulation of two-dimensional dopant redistribution in silicon, efficient numerical algorithms are necessary to solve the system of stiff nonlinear partial differential equations involved. Special problems arise because of nonplanar time-dependent geometries (e.g. in case of local oxidation) and of the need as well to resolve very shallow structures (e.g. phosphorus and arsenic implantations) as to cover large simulation areas in case of CMOS wells, bipolar structures, or defect distribution profiles with a limited number of meshpoints.

In many process simulation programs, for example LADIS (Tielert 1980), SUPRA (Chin 1982), BICEPS (Penumalli 1983), and COMPOSITE (Lorenz 1985), Finite Difference methods have been used for the

discretization of the diffusion equations. These methods are in general reasonably easy to implement but are, however, quite limited in terms of both accuracy and performance. Finite Element approaches used with other programs, e.g. SUPREM IV (Law 1988) and TITAN (Gerodolle 1985) in general need less meshpoints but are more difficult to implement and face problems with adaptive meshing.

To overcome these problems, the ASWR method discussed below is applied together with two transformations of the differential equations.

TRANSFORMATION OF THE DIFFUSION EQUATION

In general, a simulation program has to face the problem of nonplanar time-dependent geometries. On one hand, the numerical method applied to solve the diffusion equation should use a mesh which contains the boundaries of the simulation domain, e.g. the interface between oxide and silicon in case of local oxidation. On the other hand, Finite Difference methods mostly use a rectangular mesh. In COMPOSITE, a modification of the conformal mapping discussed by Seidl (Seidl 1985) is used to map the domain where the solution is to be obtained (physical domain, coordinates x, y) onto a rectangle (mathematical domain, coordinates ξ, η). The situation is shown in fig. 1. Fig. 2 shows a nonplanar bird's beak as an example of a mesh generated by the conformal mapping.

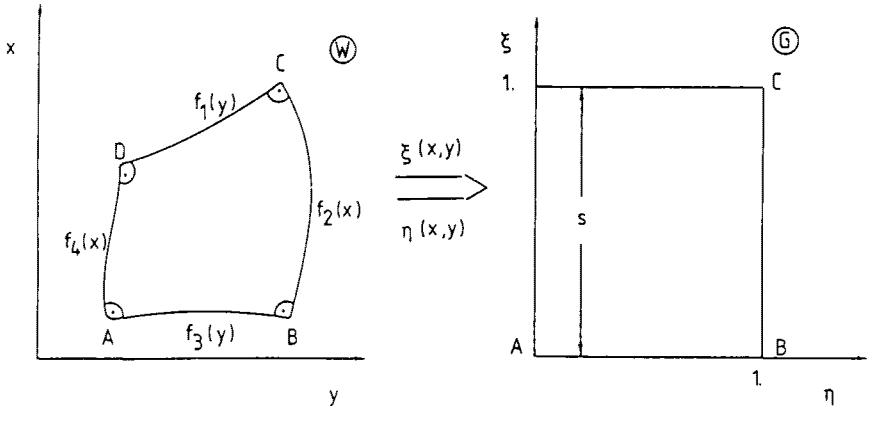

Fig. 1: Conformal mapping between a) physical domain, coordinates (x, y), b) mathematical domain, coordinates (ξ, η).

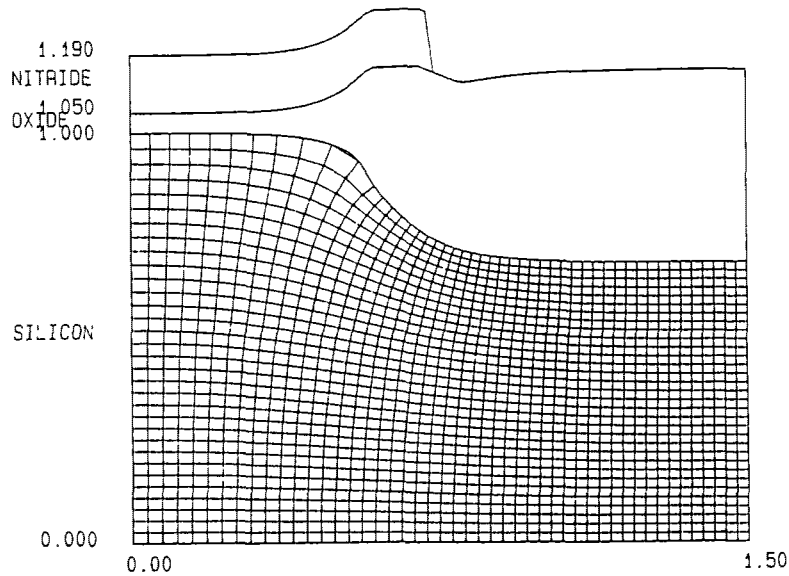

Fig. 2: Example of mesh generated by the conformal mapping: bird's beak resulting from recessed oxidation

This mapping is defined by the differential equations

(1)
$$\frac{\partial \xi(x,y)}{\partial x} = \alpha \frac{\partial \eta(x,y)}{\partial y}$$

$$\frac{\partial \xi(x,y)}{\partial y} = -\alpha \frac{\partial \eta(x,y)}{\partial x}$$

for

(2)
$$0 \leq \xi \leq 1 \text{ and } 0 \leq \eta \leq 1.$$

In (1), α is used to make sure that (2) is satisfied. In case of $\alpha = 1$, (1) reduces to Cauchy-Riemann's differential equations which define a conformal mapping. The diffusion equation for e.g. one dopant species,

(3)
$$\frac{\partial C}{\partial t} = \frac{\partial}{\partial x}(D(C)\frac{\partial C}{\partial x}) + \frac{\partial}{\partial y}(D(C)\frac{\partial C}{\partial y})$$

is transformed to yield

$$(4) \qquad \frac{\partial C}{\partial t} = [(\frac{\partial \xi}{\partial x})^2 + (\frac{\partial \xi}{\partial y})^2][\frac{\partial}{\partial \xi}(D(C)\frac{\partial C}{\partial \xi}) + \frac{1}{\alpha^2}\frac{\partial}{\partial \eta}(D(C)\frac{\partial C}{\partial \eta}))]$$

In (4), no mixed derivatives $\frac{\partial}{\partial \xi}\frac{\partial}{\partial \eta}$ occur as they cancel each other because of (1). The only modification of (4) compared with (1) is that different diffusion coefficients apply in the two directions ξ and η. In contrast to mixed derivatives, this does not introduce difficulties into algorithms used to solve the equation.

Another transformation applied with the ASWR method results from a scaling of the concentrations. Looking at 1-d Gaussian implantation profiles and linear diffusion, $D(C)$=const., the time-dependent solution of (1) would look like

$$(5) \qquad C(x,y,t) = \frac{N_{\sqcup}}{\sqrt{2\pi(\Delta R_p^2 + 2Dt)}} exp(\frac{-(x-R_p)^2}{2(\Delta R_p^2 + 2Dt)})$$

C ranges from 0 to about 10^{21}, where $\ln(C+1)$ ranges from 0 to about 48 and may be approximated much better by polynomials than C itself. Therefore, in connection with the ASWR method the transformation

$$(6) \qquad \tilde{C}(x,y,t) = ln\ C(x,y,t)$$

is used, where $C(x,y,t)$ is set to a minimum value C_{min} ($\approx 10^{12}\mathrm{cm}^{-3}$) if it decreases below that value. Equation (4) then reads

$$(7) \qquad \begin{aligned} \frac{\partial \tilde{C}}{\partial t} &= [(\frac{\partial \xi}{\partial x})^2 + (\frac{\partial \eta}{\partial y})^2][\frac{\partial}{\partial \xi}(D(\tilde{C})\frac{\partial \tilde{C}}{\partial \xi}) + \frac{1}{\alpha^2}\frac{\partial}{\partial \eta}(D(\tilde{C})\frac{\partial \tilde{C}}{\partial \eta}) \\ &+ D(\tilde{C})[(\frac{\partial \tilde{C}}{\partial \xi})^2 + \frac{1}{\alpha^2}(\frac{\partial \tilde{C}}{\partial \eta})^2]] \\ &=: L\tilde{C} \end{aligned}$$

where L is some differential operator.

Like Finite Elements, the ASWR method attempts to obtain approximative solutions of (7) in a weighted integral sense, which means $\hat{C}$ belonging to a trial function space U and satisfying

$$(8) \qquad \int (\frac{\partial \hat{C}}{\partial t} - L\hat{C}) \cdot v \, d\Omega = 0$$

where the integration domain is the simulation area and v an arbitrary function from a test function space V. In contrast to Finite Elements, for the ASWR method the spaces U and V are not equal.

In the following, a brief outline of the basic principles of the method is given. Details are discussed in (Svoboda 1988).

TRIAL AND TEST FUNCTIONS

Looking at (5), a good approximation to the logarithm of the concentration can be obtained by parabolic polynominals in both x and y, which would allow an exact approximation of (5) with only three meshpoints in horizontal and vertical direction. Even in case of more realistic implantation profiles, e.g. Pearson distributions, and nonlinear diffusion, equation (7), this approach is likely to yield a good approximation of the exact solution using only a moderate number of meshpoints. Therefore the space U of trial functions is chosen to consist of a special kind of these functions.

For the definition of 1d trial functions, first a monotonically increasing sequence $\{\tau_i\}_1^{m+3}$ is given on the interval [a,b] with $a = \tau_1 = \tau_2 = \tau_3$, $\tau_{m+1} = \tau_{m+2} = \tau_{m+3} = b$ and $\tau_i < \tau_{i+1}$ for i $\epsilon\{3, ..., m\}$. Then splines $B_i(x)$ are defined:

$$(9) \quad B_i(x) := \begin{cases} \frac{(x-\tau_i)^2}{(\tau_{i+2}-\tau_i)} & \text{for x } \epsilon \ [\tau_i, \tau_{i+1}] \\ \frac{(x-\tau_i)(\tau_{i+2}-x)}{(\tau_{i+2}-\tau_i)(\tau_{i+2}-\tau_{i+1})} + \frac{(\tau_{i+3}-x)(x-\tau_{i+1})}{(\tau_{i+3}-\tau_{i+1})(\tau_{i+2}-\tau_{i+1})} & \text{for x } \epsilon \ [\tau_{i+1}, \tau_{i+2}] \\ \frac{(\tau_{i+3}-x)^2}{(\tau_{i+3}-\tau_{i+2})(\tau_{i+3}-\tau_{i+1})} & \text{for x } \epsilon \ [\tau_{i+2}, \tau_{i+3}] \end{cases}$$

From these 1d splines, 2d splines are defined according to

$$(10 \text{ a}) \qquad \tilde{B}_{kl} := \frac{1}{hy_l} \int_{y_l}^{y_{l+1}} B_k(y) dy \quad \text{with } hy_l := y_{l+1} - y_l$$

$$(10 \text{ b}) \qquad \tilde{B}_{ij} := \frac{1}{hx_j} \int_{x_j}^{x_{j+1}} B_i(x) dx \quad \text{with } hx_j := x_{j+1} - x_j$$

where τ from eq. (9) has been replaced by x and y, respectively, and

$$D_{ik}(x,y)|_{\Omega_{jl}} := \bar{B}_{kl}B_i(x) + \tilde{B}_{ij}B_k(y) - \bar{B}_{kl}\tilde{B}_{ij} \tag{11}$$

where Ω_{jl} are the boxes in the mathematical domain, see fig.3. hy_l and hx_j are the mesh spacings of the mathematical domain in vertical and horizontal direction, respectively. In general, a trial function may now be written as

$$u = \sum_{ik} b_{ik} D_{ik}(x,y) \tag{12}$$

with coefficients b_{ik}.

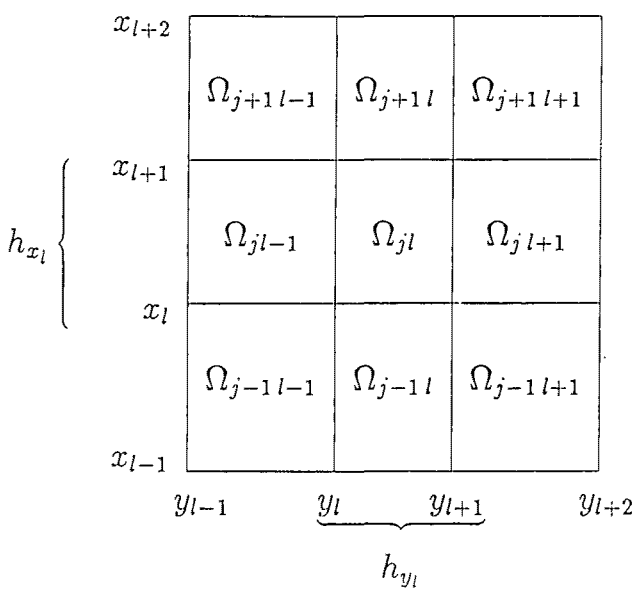

Fig. 3: Subset of boxes in the mathematical domain.

From (9) and (10) it results that D_{jl} equals zero outside the 9 boxes displayed in fig. 3. In addition, as well the integrals of D_{ik} as its normal derivatives along each side of a box are continous.

The space of test functions is now chosen to consist of all functions which are constant on a box. Base functions are

$$\{v_{ik}|v_{ik}(x,y) = \begin{cases} 1 & \text{for (x,y)} \ \epsilon \ \Omega_{\text{ik}} \\ 0 & \text{else} \end{cases} \} \tag{13}$$

Using eqs. (9) to (13), (8) results in a system of nonlinear equations for the coefficients b_{ik} of eq. (12). As each D_{ik} is equal to zero outside an area of 3 x 3 boxes, each of these equations reveal a band structure with 9 elements in each line being different from zero. This system of nonlinear equations is solved, taking into account the nonlinearities implicity.

ADAPTIVE MESH

During diffusion, regions of the dopant profile which must be discretized with a fine mesh spacing move considerably. Therefore, either a lot of meshpoints or a mesh which moves according to the dopant profile must be used to ensure accuracy of the numerical solution.

At each time step, this mesh is a rectangular one in the mathematical domain with an additional point in the center of each box. In the examples, fig. 2 and fig. 4, a refinement of these meshes is displayed which results from adding the midpoints of the sides of the boxes in order to use a simple rectangular mesh with the plot module.

The basic idea of the mesh adaptation method implemented is that the error in the space approximation in each direction with splines (order l) may be minimized by demanding an equidistribution of

$$F_l := h_i^{l+1} |u^{(l+1)}(x_i)| = \text{const} \tag{14}$$

where h_i is the local meshsize and $u^{(l+1)}$ is the $(l+1)^{\text{th}}$ derivative of the exact solution (Pereyra 1975). Focusing on the time discretization, an equidistribution of the error of the electrical potential, treating each direction seperately, turns out to be appropriate:

$$F_2 := h_i^2 |\Phi''_i| = \text{const}, \quad i = 1, ..., n. \tag{15}$$

With the ASWR-implementation used in COMPOSITE, (15) is used as the default rule to control the mesh. In detail, new meshlines are introduced wherever F_2 exceeds 4 times its mean value. Doing this, the algorithm tries to take these meshlines from areas where F_2 is less than 25% of its mean value. This method is also applied to create the initial mesh when introducing a doping into the wafer for the first time, e.g. in case of ion implantation. Here, an estimate of the doping profile after the implantation is calculated, and the adaptive mesh algorithm is applied to this profile. The actual implantation is then performed onto the adaptive mesh. An example is given below.

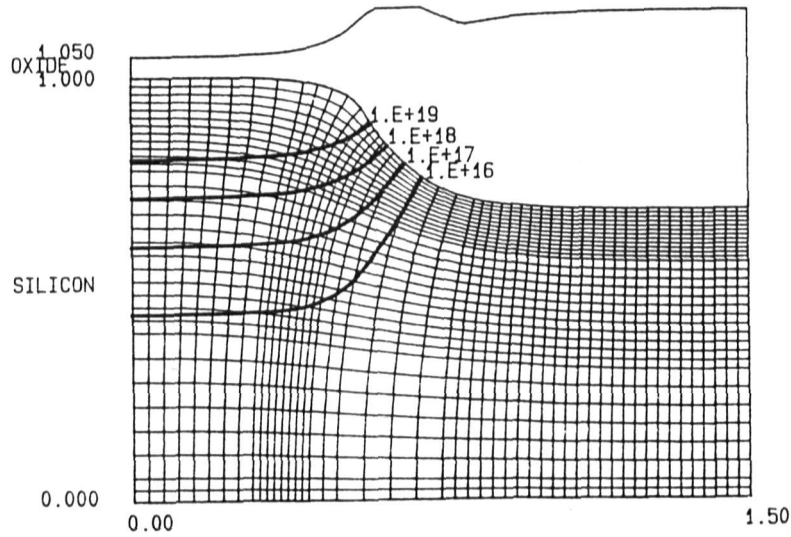

Fig. 4a: Adaptive mesh and boron equiconcentration line plot after implantation of a dose of $10^{15}cm^{-2}$ boron at an energy of 40 keV.

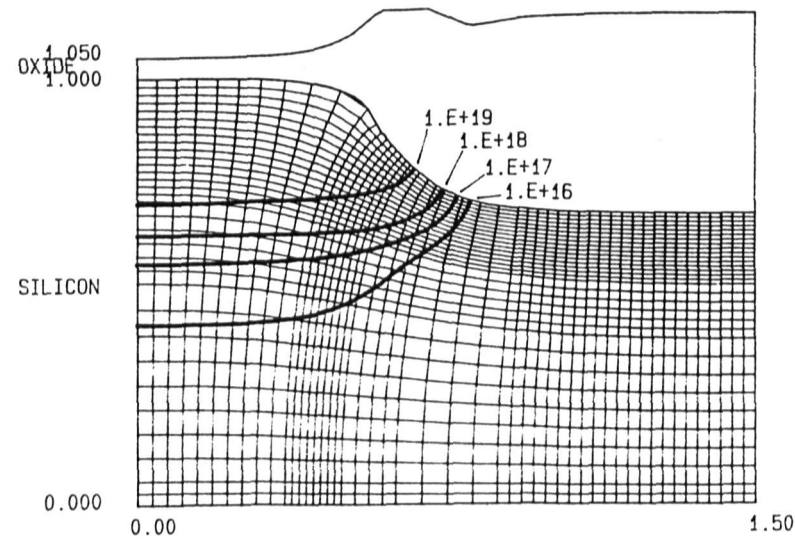

Fig. 4b: Adaptive mesh and boron equiconcentration line plot after inert diffusion at 1000°C for 30 min.

TIME STEP CONTROL

Different from the usual Finite Difference methods, the total amount of dopant in the wafer is not automatically conserved in case of Neumann boundary conditions. Here, the error in the total mass is related to the discretization error of the concentration in time and space. Therefore, with the ASWR-implementation used in COMPOSITE, the error in the total mass is used to control the time step size.

EXAMPLES

In fig. 4, the change of the adaptive mesh during ion implantation and a subsequent diffusion step is shown. The initial geometry has been an oxide mask processed by recessed oxidations which was simulated by COMPOSITE, see fig. 2. A dose of $10^{15}cm^{-2}$ boron is implanted at an energy of 40 keV and then diffused at 1000°C for 30 min. Fig. 4a and b show the adaptive meshes and an equiconcentration line plot of the boron profile after the ion implantation and the diffusion, respectively.

In this example, a calculation of the diffusion step with the Finite Differences method previously used in COMPOSITE takes about 4 times the computation time of the nonoptimized ASWR-solution. For longer diffusion times, the speedup of the ASWR increases. With some examples, a speedup 100 and more has been observed.

In fig.5, mountain plots of the result of a coupled diffusion (1000°C 5 min) of high concentration arsenic and boron are shown. In fig. 5a and 5b, the arsenic and boron profiles after the diffusion step are shown as they were calculated using ASWR and the adaptive mesh. Large changes in the mesh spacings appear both in vertical and horizontal direction, especially near the 2-d pn-junction. In fig. 6, the boron profile calculated with an equidistant mesh is shown. Here, especially the pn-junction is only poorly resolved.

CONCLUSION

An ASWR method for the simulation of dopant redistribution in silicon has been developed and implemented in COMPOSITE. It contains an adaptive mesh algorithm and is able to solve diffusion problems with less mesh points and higher accuracy than Finite Difference approaches. Compared with the SOR solver previously used in COMPOSITE, the speedup depends strongly on the application. A raw estimate is one order of magnitude. Further possible developments of the method are the application of a more advanced linear equation solver, and vectorization.

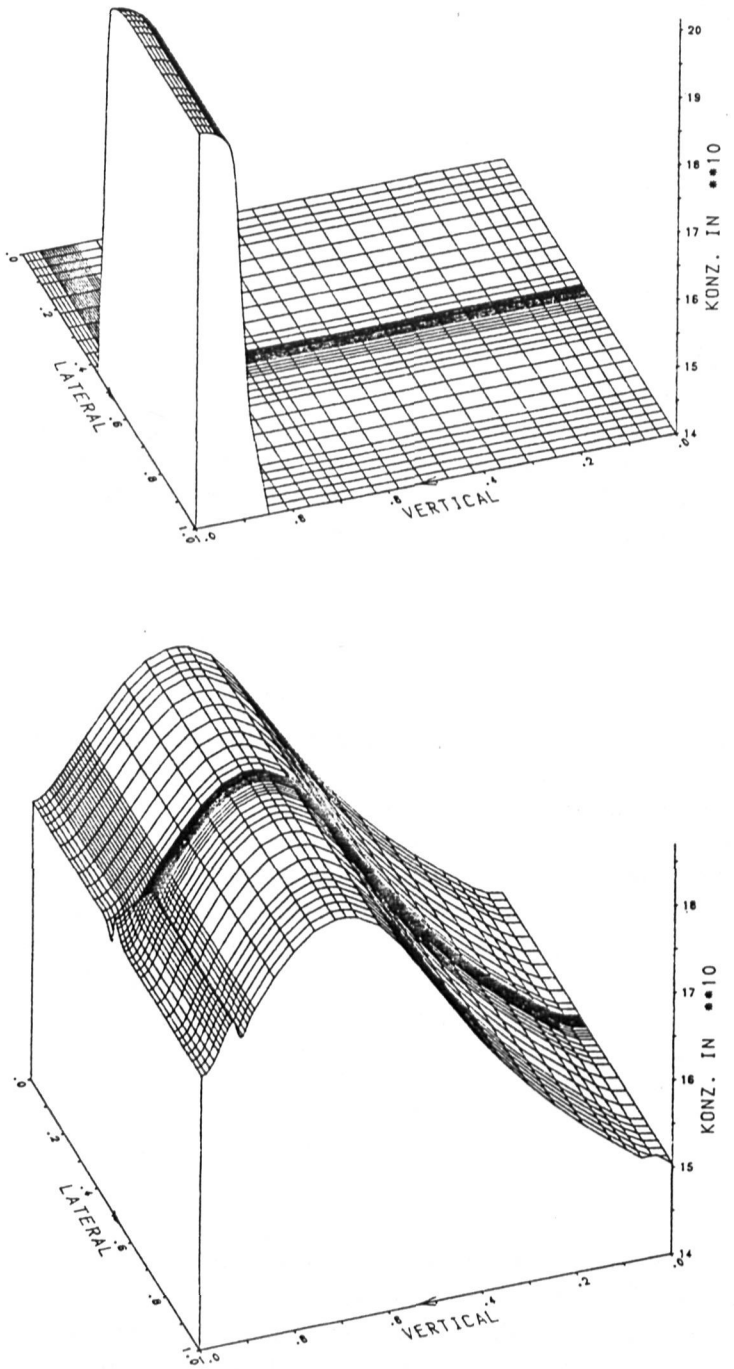

Fig. 5: Mountain plot of dopant concentration after a coupled diffusion of boron and arsenic at 1000 °C for 5 min simulated with ASWR and adaptive mesh: a) arsenic profile, b) boron profile

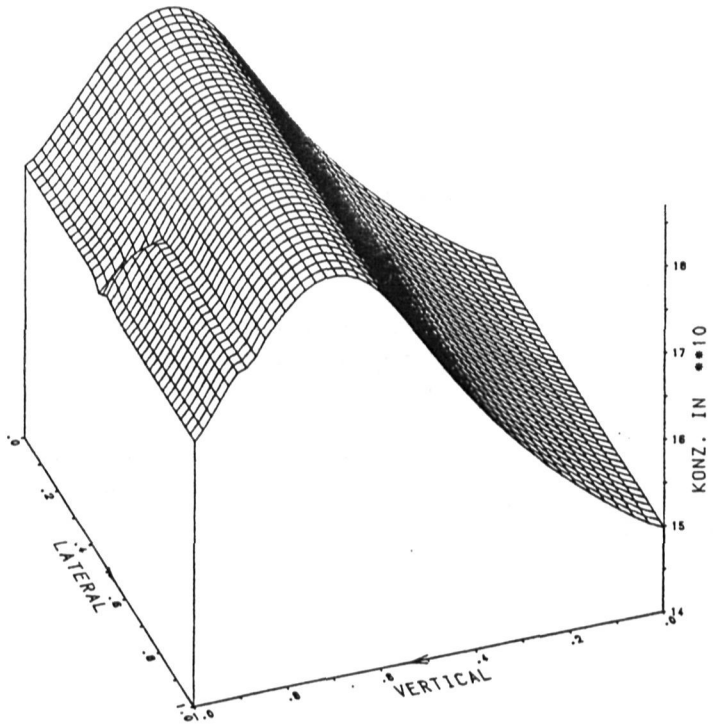

Fig. 6: Mountain plot of boron concentration after a coupled diffusion of boron and arsenic at 1000 °C for 5 min simulated with an equidistant mesh.

REFERENCES

Chin D., Kump M.R., Lee H.G. and Dutton R.W. (1982). *Process design using two dimensional process and devices simulators.* IEEE Trans. Electron Devices ED-29, 336-340

Gerodolle A., Martin S. and Marrocco A. (1985).*Finite element method applied to 2D MOS process simulation and defect diffusion: program TITAN.* Proc. NASECODE IV, Boole Press, Dublin, 287-292

Law M.E. and Dutton R.W. (1988). *Verification of Analytic Point Defect Models Using SUPREM-IV.* IEEE Trans. CAD, CAD-7(2), 181-190

Lorenz J., Pelka J., Ryssel H., Sachs A., Seidl A. and Svoboda M. (1985). *COMPOSITE - A complete Modeling Program of Silicon Technology.* IEEE Trans. Electron Devices ED-32(10), 1977-1986

Penumalli B.R (1983). *A comprehensive two-dimensional VLSI process simulation program, BICEPS.* IEEE Trans. Electron Devices ED-30 (9), 986-992

Pereyra V. and Sewell E.G. (1975). *Mesh selection for discrete solution in ordinary differential equations.* Numer. Math. 23, 261-268

Seidl A. and Svoboda M. (1985). *Numerical Conformal Mapping for Treatment of Geometry Problems in Process Simulation.* IEEE Trans. Electron Devices ED-32 (10), 1960-1963

Svoboda M. (1988). *Ein Petrov-Galerkin-Verfahren zur Simulation der Festkörperdiffusion in der Halbleiterherstellung.* Ph-D thesis, Ludwig-Maximilians-Universität, München

Tielert R. (1980). *Two dimensional numerical simulation of impurity redistribution in VLSI processes.* IEEE Trans. Electron Devices ED-27 (8), 1479-1483